Electronic Supplementary Material (ESI) for ChemComm.

Electronic supplementary information

Quantitative investigation of CeO_2 surface proton conduction in H_2 atmosphere

Taku Matsuda, Ryo Ishibashi, Yoshiki Koshizuka, Hideaki Tsuneki, Yasushi Sekine*

Department of Applied Chemistry, Waseda University, 3-4-1, Okubo, Shinjuku, Tokyo, 169-8555, Japan, *E-mail: ysekine@waseda.jp

Experimental procedures

Sample preparation

In this study, we used a CeO_2 powder (purity:99.99%) supplied by the Catalysis Society of Japan. The powder has been prepared by calcinating cerium carbonate at 573 K. Then, we prepared CeO_2 pellets for AC impedance measurements by following procedure; first, the CeO_2 powder suspended in isopropanol was ground to fine particles in a planetary mill (pulverisette 6; Fritsch GmbH). Grinding was carried out at 300 rpm for 15 min, paused for 10 min and re-ground while rotating backwards at 300 rpm for 15 min. After removal of isopropanol, the CeO_2 fine powder was pressed at 100 kN for 2 min. The resulting pellets were then sintered in air at 1073 K for 2 h at a temperature increase rate of 5 K min^{-1}. The diameter and thickness of the sintered pellets were 16.75 mm and 0.95 mm, respectively. The relative density measured by the geometric method was about 60%.

AC impedance measurement

Circular platinum electrodes (thickness of about 100 nm and a diameter of 11.25 mm) were deposited on both side of the pellet by magnetron sputtering using MSP-20UM (VACCUM DEVICE, Japan) and used for the measurements. Conductivity was investigated by AC impedance measurement using a two-electrode, four-wire setup with a ZG4 interface connected to an alpha-A high-performance frequency analyzer (Novocontrol Technologies). A temperature-controlled ProbostatTM (NorECs AS, Norway) was used as the measuring cell under a gas flow of 30 SCCM in the frequency range from 1 MHz to 1 mHz with an amplitude of 0.5 to 1.5 V. All measurements were performed under dry gas environment. The gas purity, impurities, dew point, relative humidity at room temperature (293 K) were listed in Table S1. The relative humidity was calculated from the dew point. Prior to measurement, surface adsorbed species were removed under Ar flow at 773 K. Pre-treatment was continued until the electrical conductivity was stabilized. Next, H_2 pre-treatment was carried out for 2 h at 573 K under 20%H_2/Ar flow, followed by Ar purging at 573 K to remove adsorbed H_2. After pre-treatment, the following measurements were performed. First, the temperature dependence of conductivity was measured under Ar flow at 423-723 K and under 5%H_2/Ar flow at 423-573 K. To further confirm the effect of adsorbed species, the H/D isotope effect was investigated using 5%D_2/Ar at 423-573 K. Finally, the H_2 partial pressure (P_{H2}) dependence of conductivity was evaluated in the P_{H2} region of 5.1×10^{-4} to 4.9×10^{-2} atm (Ar dilution) at 473 K. All impedance spectra under H_2(D_2) flow were recorded 30 min after H_2 (or D_2) supply. The measured impedance spectra were analyzed and fitted using an equivalent circuit model with a parallel RQ circuit presented in Fig. S1. using the software ZView (Scribner Associates, USA). The conductivity was calculated according to Equation (1), where *R* is

the resistance obtained, *L* is the thickness of the pellet and *S* is the area of the platinum electrode.

$$\sigma = \frac{1}{R}\frac{L}{S} \tag{1}$$

Table S1 Gas purity, impurities, dew point, and relative humidity

Gas	Purity	Impurities						Dew point	Relative humidity (298 K)
		N_2	O_2	H_2	CO	CO_2	THC		
-	vol.%	vol.ppm	vol.ppm	vol.ppm	vol.ppm	vol.ppm	vol.ppm	K	%
Ar	>99.995	<0.5	<0.2	<0.5	<0.2	<0.2	<0.2	<193	<0.004
H_2	≧99.99	≦80	≦3	-	≦0.5	≦0.5	≦1.0	<213	<0.061

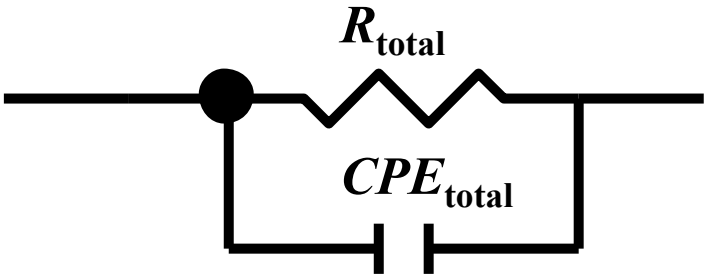

Fig. S1 Equivalent circuit used for analysis:

R and CPE denotes resistance and constant phase element respectively.

H_2-TPR measurement

Reduction behavior of the CeO_2 with Pt electrodes was investigated by H_2-TPR using BELCAT II (MICROTRAC, Japan). The CeO_2 pellet with Pt electrodes was crushed into a powder for the measurement. Then, the powder (50 mg) was pretreated under Ar flow at 773 K for 0.5 h. After the sample cooled to 323 K, 5%H_2/Ar was introduced into the sample at a flow rate of 30 SCCM. Then, the temperature was increased up to 1173 K at a rate of 10 K min^{-1}.

SEM measurement

The morphology of the sintered pellet was analyzed by SEM using JSM-IT100 (JEOL, Japan) with 20 kV acceleration voltage on Pt-Pd alloy coated sample.

XRD measurement

The crystal structures of CeO_2 starting powder and sintered sample were investigated by XRD using SmartLab 3 (Rigaku, Japan). XRD patterns were measured using a λ = 1.5418 Å with Cu-K_α radiation.

Results and Discussion

On the possible contribution of oxygen loss and electronic conduction by H_2 supply

H_2 supply may cause not only surface proton conduction but also oxygen vacancy formation, resulting in the enhancement of the electronic conduction. However, we do not attribute the enhancement of the conductivity during H_2 supply to oxygen loss and electronic conduction based on the following experimental results. First, we investigated the electrical conductivity for porous CeO_2 under Ar atmosphere before and after H_2 pre-treatment and Ar purging. As presented in Fig. S2, there was almost no changes in the electrical conductivity before and after the pre-treatment. The result indicated that the increase in conductivity during H_2 supply returns to its original value by Ar purging. Such reversibility of the electrical conductivity cannot be explained by oxygen loss and enhanced electronic conductivity since oxygen loss is irreversible unless oxidant is supplied. Next, we performed H_2-TPR measurement for the CeO_2 sample to investigate the reduction behaviour. H_2-TPR profile depicted in Fig. S3 showed few amounts of H_2 consumption below 800 K, which means that oxygen loss during H_2 supply was negligibly small.

According to these results, we concluded that the marked increase in conductivity during H_2 supply is not attributable to oxygen vacancy formation.

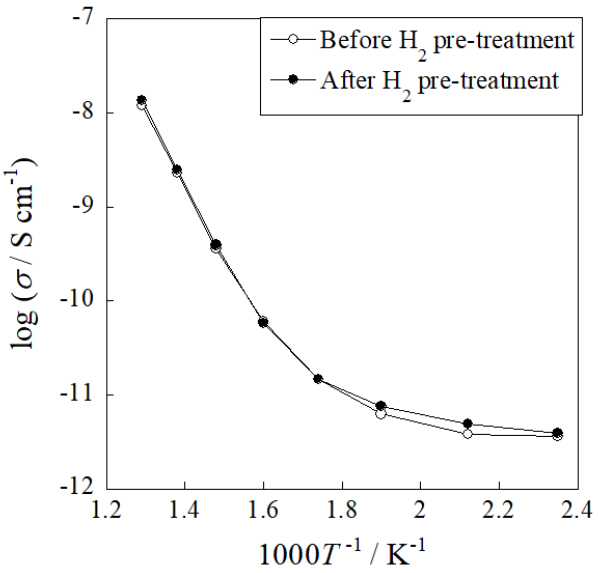

Fig. S2 Temperature dependence of electrical conductivity for CeO_2 under Ar atmosphere before and after H_2 pre-treatment and Ar purging.

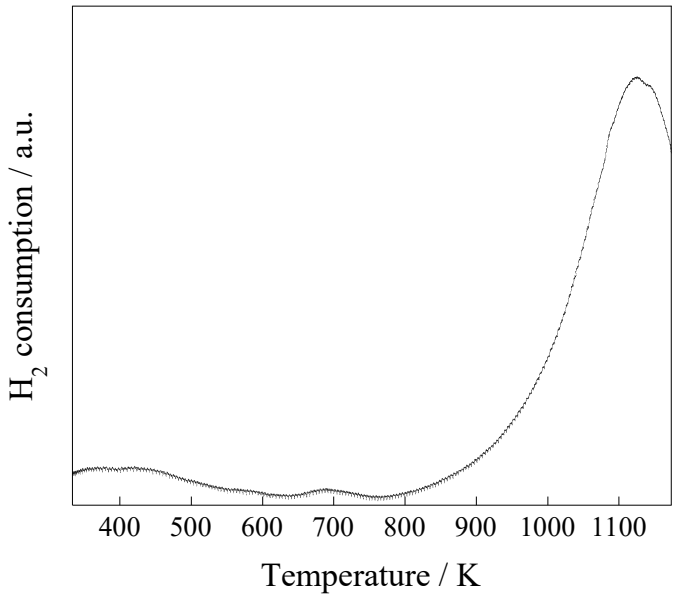

Fig. S3 H_2-TPR profile for a CeO_2 sample with Pt electrodes.

SEM: Observation of microstructure of sintered CeO_2 pellet

SEM measurements were carried out to observe the microstructure of sintered CeO_2 pellet. As presented in Fig. S4 the SEM images of CeO_2 showed numerous pores, indicating a large number of available adsorption sites. In such porous sample, adsorption of H_2O or H_2 can highly affect the surface electrical properties.

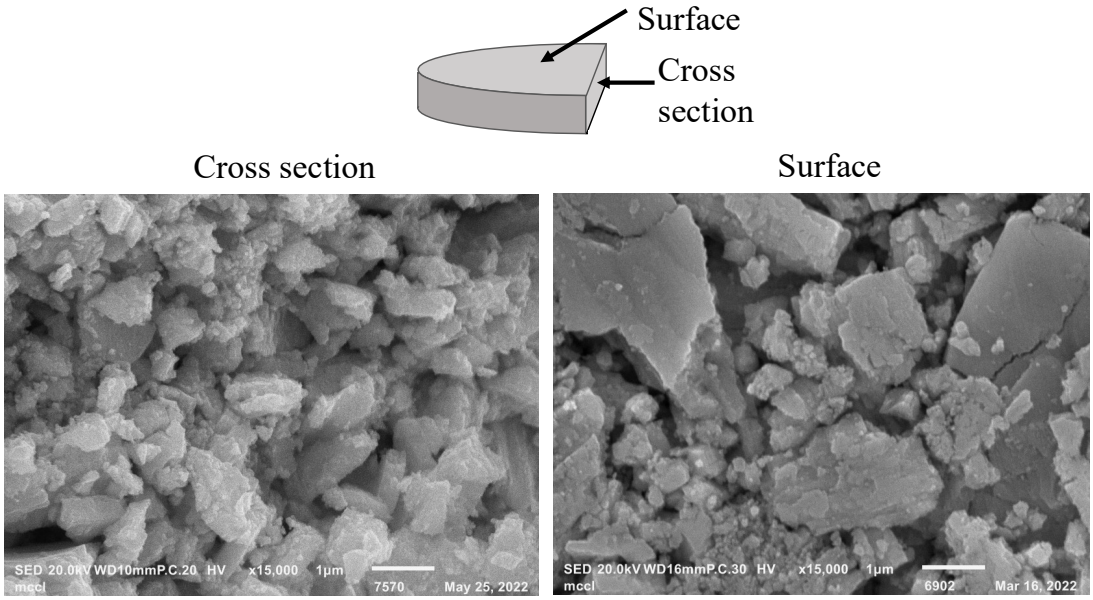

Fig. S4 SEM images of CeO_2: cross section and surface

H/D isotope effect on conductivity

Temperature dependences of electrical conductivity for CeO_2 under 5%H_2/Ar and 5%D_2/Ar atmospheres are shown in Fig. S5.

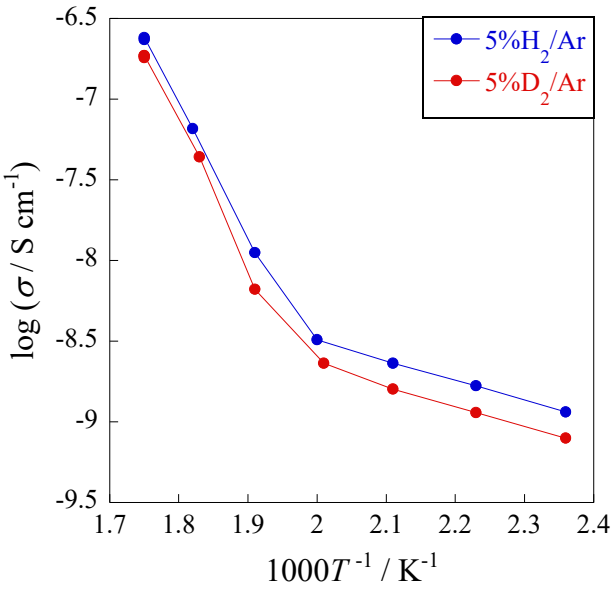

Fig. S5 Temperature dependences of electrical conductivity for CeO_2 under 5%H_2/Ar and 5%D_2/Ar atmospheres.

On the possible contribution of water vapor in H_2

We provided clear evidence that H_2 introduction enhances the electrical conductivity. However, there may be a possible contribution of water vapor in H_2. Regarding that, we do not attribute the enhancement of conductivity by H_2 supply to water vapor in hydrogen due to the following reasons. First, measured H/D isotope effects strongly deny the possibility that the water vapor mainly contributed the conduction. H/D isotope effects should not appear if protons are generated not by H_2/D_2 but water vapor. Second, as shown in Table S1, water

vapor contained in the gas is so small that it can unlikely increase surface proton conductivity by several orders of magnitude. Considering the reported relative humidity or water partial pressure dependence of surface proton conductivity[1),2)], the contribution of such low amount of water content can be regarded as negligible compared to that of H_2. According to the above considerations, we suppose that H_2 dissociative adsorption produces protons resulting in occurrence of surface proton conduction.

XRD: Comparison of crystal structures of CeO_2 starting powder and sintered sample

XRD measurements were conducted to assure that the crystal structure of CeO_2 was not affected by sintering at 1073 K. XRD patterns of CeO_2 starting powder and sintered sample are presented in Fig. S6. The XRD spectrum showed that both samples had a single phase assigned to CeO_2 cubic fluorite structure, indicating no changes in the crystal structure after the sintering.

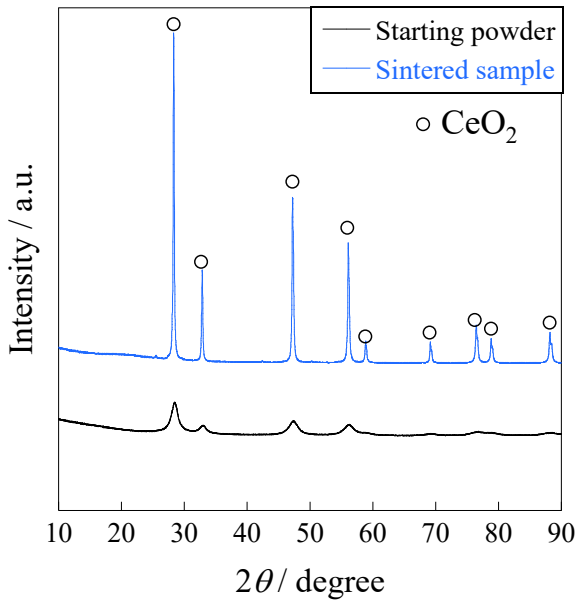

Fig. S6 XRD patterns of CeO_2 starting powder and sintered sample.

Comparison of impedance spectra with and without H_2 supply

Impedance spectra with and without H_2 supply were compared. An example of Nyquist plots and bode plots with and without H_2 supply (P_{H2} = 5.1 x 10^{-4} atm) measured at 473 K is shown in Fig. S7 and S8. Only one semicircle was observed in Nyquist plot in regardless of H_2 supply, indicating that the sample is electrically homogeneous. On the other hand, it is noteworthy that even the super-diluted H_2 supply decreased the semicircle drastically. H_2 supply also changed the frequency dependence of impedance from 1-10^{-2} Hz to 10^{2}-1 Hz as presented in the bode plots.

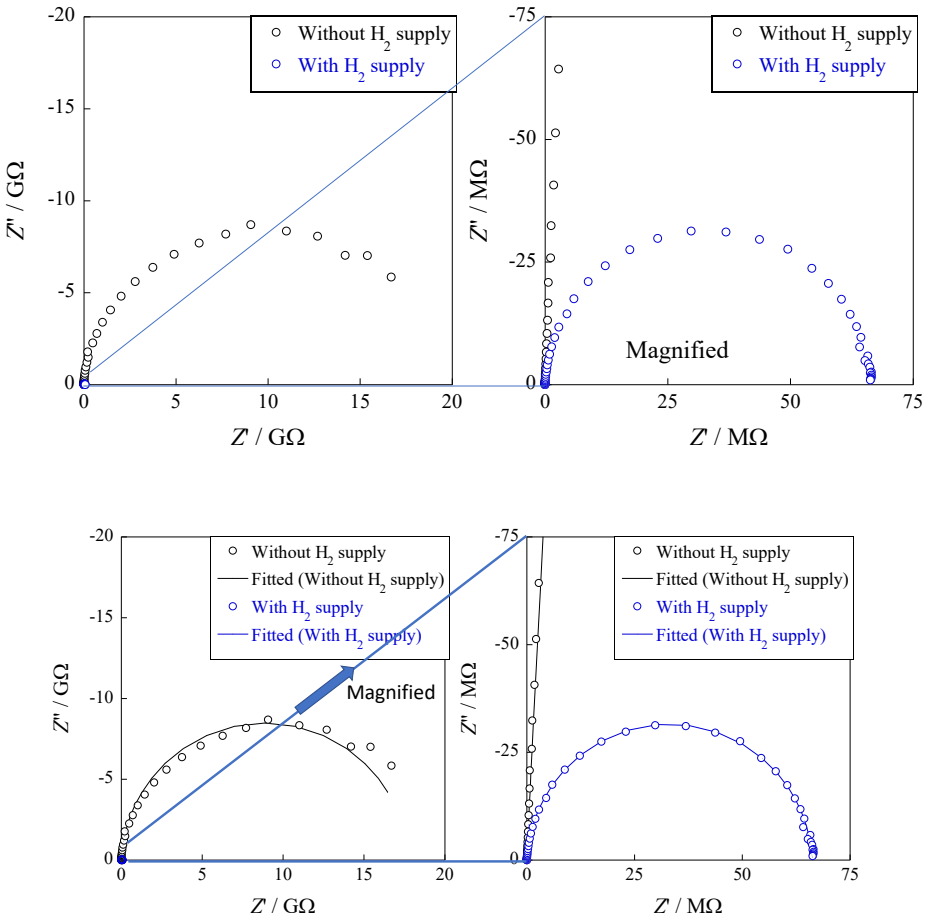

Fig. S7 Nyquist plots: Comparison of impedance spectra with and without H_2 supply (P_{H2} = 5.1×10^{-4} atm) measured at 473 K.

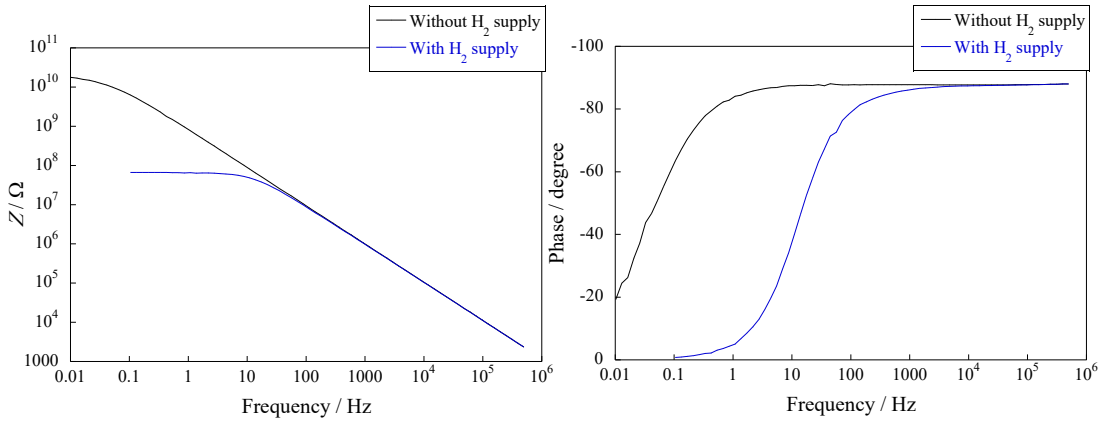

Fig. S8 Bode plots: Comparison of impedance spectra with and without H_2 supply (P_{H2} = 5.1×10^{-4} atm) measured at 473 K.

Changes in impedance over time during H_2 supply

Changes in the impedance over time during H_2 supply at 473 K were recorded for 30 minutes at a frequency of 1 Hz which corresponds to a low frequency intercept in Nyquist plot. As shown in Fig. S9, H_2 supply caused drastic decreases in the impedance at first and then the decrease in impedance became gradual. This tendency was independent of H_2 partial pressure. The results can be interpreted as follows. First, once supplied H_2 reaches to the sample, rapid formation of protons proceeds *via* dissociative adsorption of H_2 and spillover, which results in the drastic decrease in the impedance. Then, the proton formation reaches to near equilibrium, causing gradual and slow decrease in the impedance.

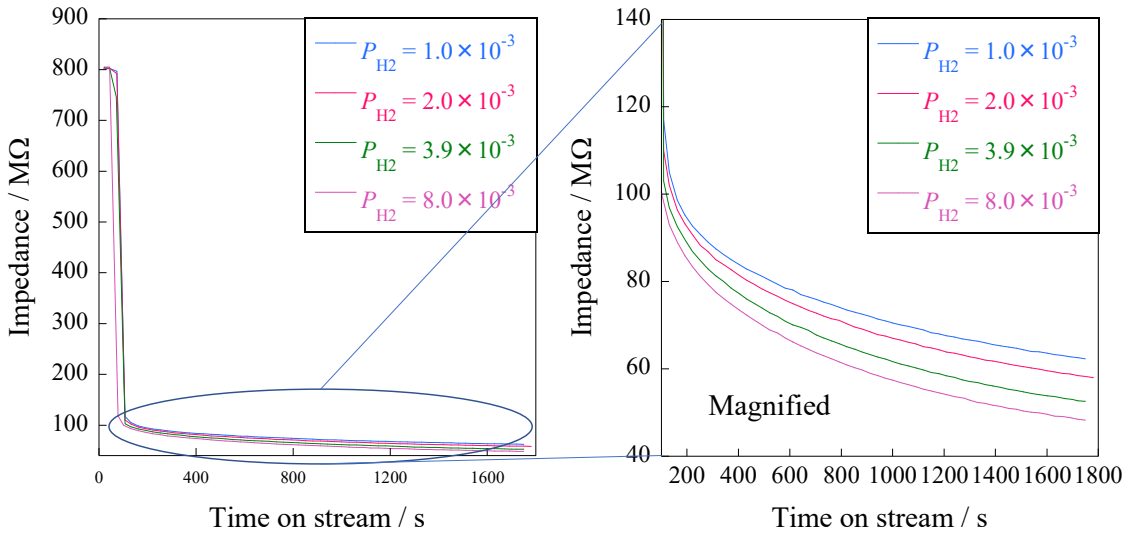

Fig. S9 Changes in impedance over time during H_2 supply at 473 K recorded at a frequency of 1 Hz.

Changes in impedance over time during Ar purge

Following AC impedance measurements under H_2 atmosphere, Ar purge was carried out to eliminate the adsorbed H_2. During the Ar purge, changes in impedance over time were recorded at a frequency of 0.1 Hz. Note that the used frequency was not 1 Hz but 0.1 Hz since it was more suitable to follow the change in impedance under Ar atmosphere. As presented in Fig. S10, an opposite tendency against the changes in impedance during H_2 supply was observed. It showed first gradual increase in impedance, followed by the sudden increase. The results can be interpreted as follows. First, H_2 desorption proceeds by recombination of protons during Ar purge, causing the gradual increase in the impedance. Then, the concentration of protons on CeO_2 surface became insufficient for proton conduction, resulting in the change in conductive carrier and sudden increase in impedance.

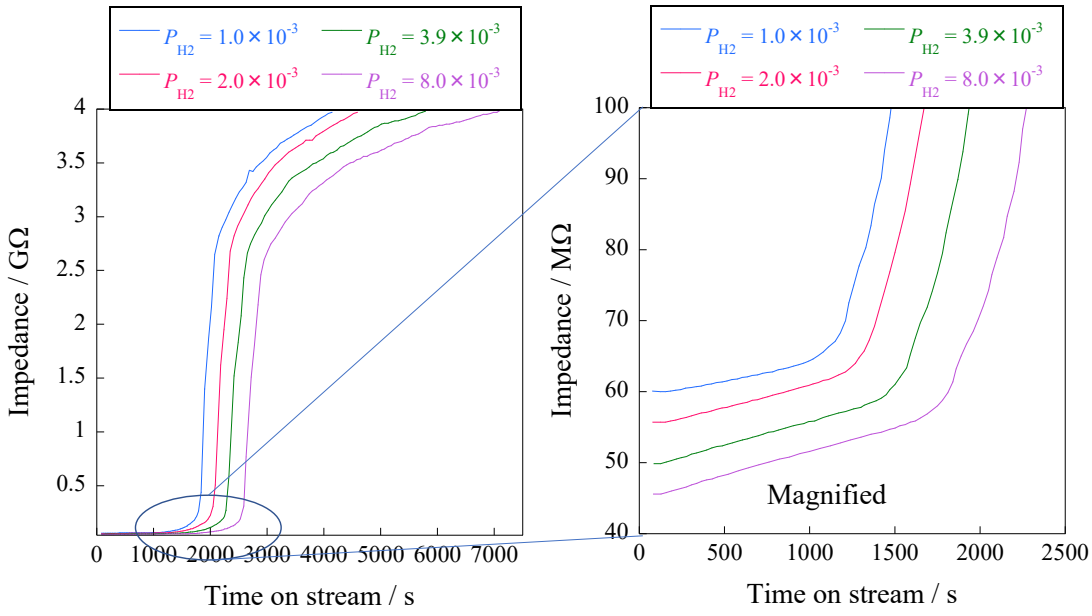

Fig. S10 Changes in impedance over time during Ar purge at 473 K recorded at a frequency of 0.1 Hz after the measurements under H_2 atmosphere.

Reproducibility of AC impedance measurements under H_2 atmosphere

In this study, AC impedance measurements were conducted 30 minutes after H_2 supply since it was difficult to achieve a steady state in the conductivity under H_2 atmosphere as indicated above. To confirm the validity of the measurements, we assessed the reproducibility. The procedure was as follows. First, we supplied H_2 for 30 minutes and then conducted AC impedance measurements. Next, we performed Ar purge until the electrical conductivity become its original value. After that, we carried out the same measurements under H_2 atmosphere again. Examples of reproducibility of the measurements are presented in Fig. S11-13. The results showed a good reproducibility, assuring the validity of the measurements. The data recorded several times are plotted in every figure. (Note that the plots appear one due to the overlapping.)

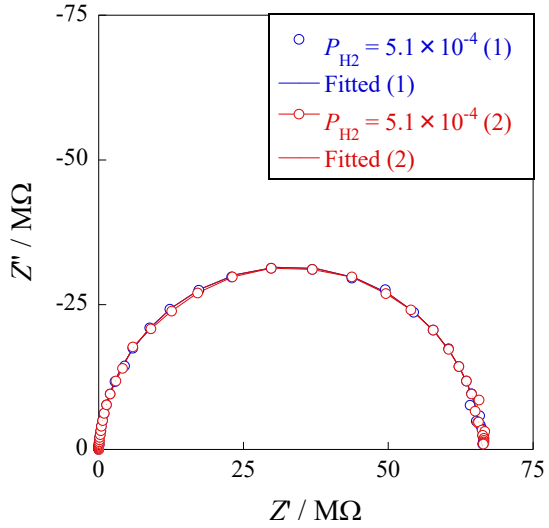

Fig. S11 An example of the reproducibility of the AC impedance measurements obtained at 473 K under H_2 supply (P_{H2} = 5.1×10^{-4} atm).

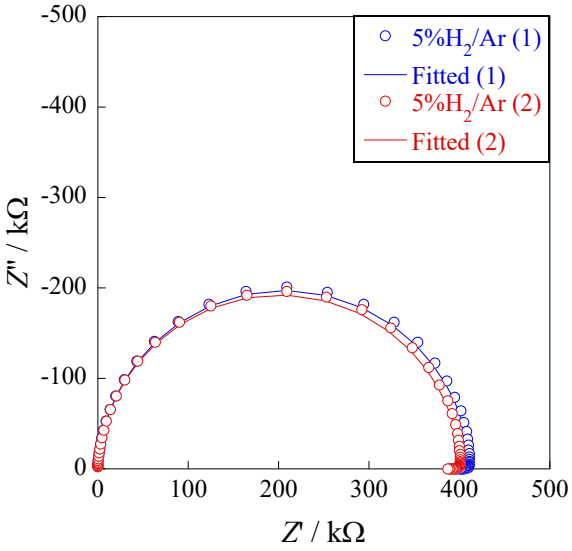

Fig. S12 An example of the reproducibility of the AC impedance measurements obtained at 573 K under H_2 supply (5%H_2/Ar).

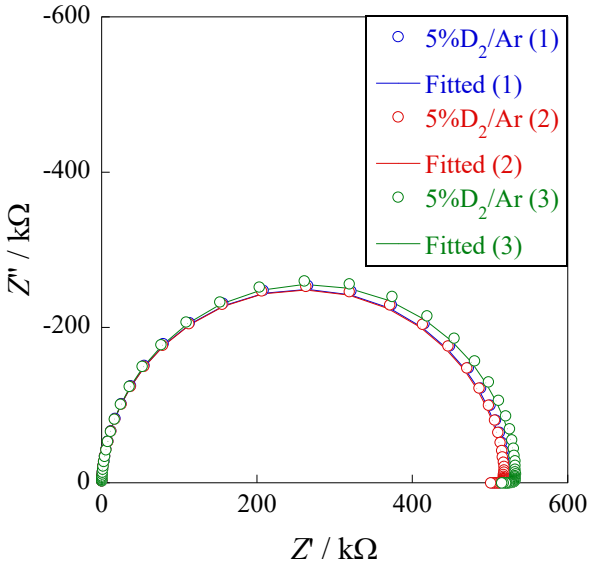

Fig. S13 An example of the reproducibility of the AC impedance measurements obtained at 573 K under D_2 supply (5%D_2/Ar).

H_2 partial pressure dependence of the coverage

The coverage for CeO_2 at each H_2 partial pressure at 473 K was calculated by the equation (10). As shown in Fig. S14, the coverage increased with H_2 partial pressure and gradually became saturated. As expected, the trend was quite similar with the H_2 partial pressure dependence of the electrical conductivity.

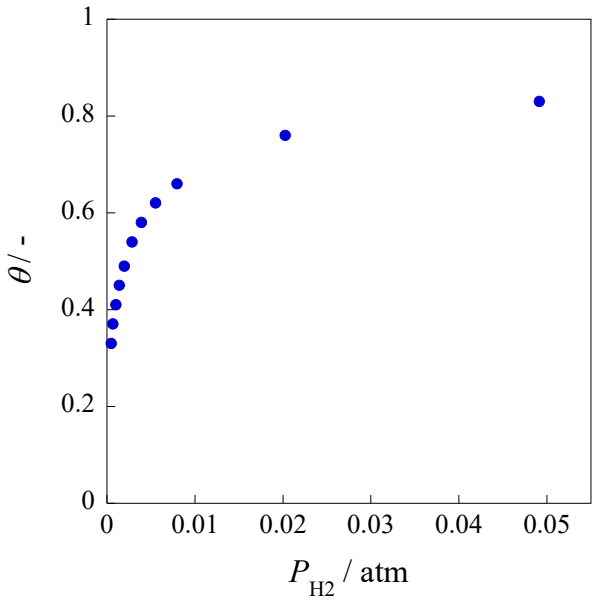

Fig. S14 Calculated coverage at each H_2 partial pressure for CeO_2 at 473 K.

Capacitance data

Capacitances measured at each condition are shown in Fig. S15-16.

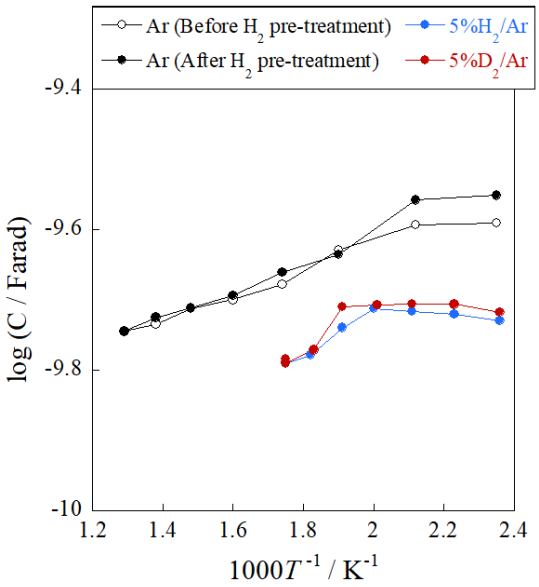

Fig. S15 Temperature dependence of capacitance for CeO_2 under Ar, 5%H_2/Ar, and 5%D_2/Ar atmosphere.

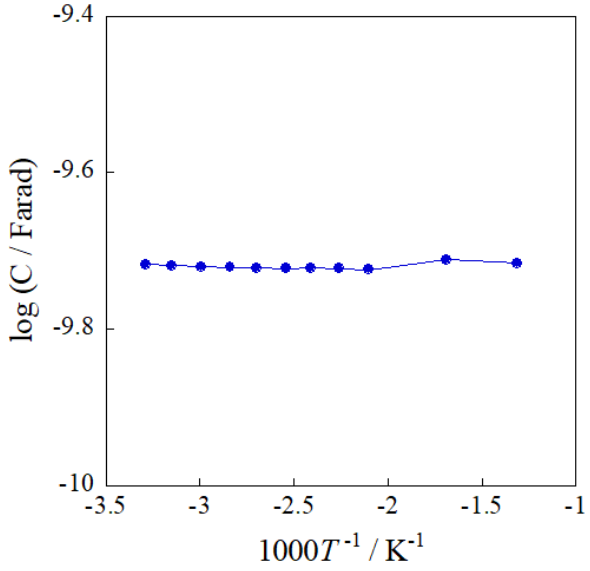

Fig. S16 Hydrogen partial pressure dependence of capacitance for CeO_2 at 473 K.

References

1. R. Manabe, S. Ø. Stub, T. Norby and Y. Sekine, *Solid State Commun.*, 2018, 270, 45-49.

2. S.Ø. Stub, E.Vøllestad, and T. Norby, *J. Phys. Chem. C*, 2017, 121(23), 12817-12825.